On the number and location of zero-group-velocity modes

Journal of the Acoustical Society of America 131 (5), May 2012, 3601-3610

On the number and location of zero-group-velocity modes

by

Eduardo Kausel[1]

Abstract

Although fundamental concepts in elastodynamics and acoustics such as waves guides, Rayleigh-Lamb modes, phase and group velocity, or anomalous modes are very well-understood and firmly established, by contrast an intense literature search in the matter of the number of zero group velocity (ZGV) modes, their location in wavenumber spectra other than at cutoff frequencies, or the methods needed to find these from first principles turned out curiously empty. Thus, this has provided the motivation for this article documenting a theoretical and quantitative analysis of this problem for horizontally layered media bounded by any arbitrary combination of external boundaries.

Introduction

It is well known that among the Rayleigh-Lamb modes in waveguides there exist a handful of branches in the low frequency-wavenumber spectrum which stand out for their anomalous characteristics, namely their phase velocity is positive while their group velocity is negative. These branches terminate at saddle points intersected by complex (evanescent) branches at which the group velocity –but not the phase velocity– vanishes altogether, and after this so-called ZGV point, a normal branch ensues for which both the group and phase velocities turn positive and thus normal. Although a rich literature exists and numerous papers have documented and evaluated these ZGV modes both numerically (Mindlin, 1958a) and in experiments which have established their unequivocal physical presence as resonances [3-6], no work to date seems to have examined how many of these modes exist or how they are distributed in $\omega - k$ space. This has given motivation for this article, documenting a theoretical and quantitative analysis to this problem not only for homogeneous plates in plane strain with free boundary conditions at its two bounding surfaces, but also for layered media bounded by any arbitrary combination of Neumann and Dirichlet boundaries.

ZVG modes in an arbitrarily layered system

Consider a horizontally homogeneous medium of finite thickness h characterized by a depth-dependent shear modulus $\mu(z)$, Lamé constant $\lambda(z)$ and mass density $\rho(z)$. With appropriate use of singularity functions, this description also can be made to include layered media for which the properties are locally homogeneous but change abruptly from layer to layer. Also, the medium is bounded by any arbitrary combination of clamped (Dirichlet) and/or free (Neumann) boundaries at its two horizontal, external surfaces. We designate these boundary conditions by two pairs of indices such as FF-FF, FF-CC, FC-CF, and so forth, with the first index in each pair referring to the normal (vertical) condition, and the second to the tangential (horizontal) condition. Also, the first pair refers to the upper boundary while the second pair identifies the lower boundary. For

[1] Professor of Civil and Environmental Engineering, Massachusetts Institute of Technology, Cambridge, MA 02139

example, a wholly free plate has FF-FF boundaries. As has already been amply documented in the technical literature over the past century, any such system admits a family of real (i.e. non-evanescent) propagation modes which define the frequency-wavenumber spectrum. These are occasionally supplemented by complex wavenumber branches that represent evanescent modes, of which there are infinitely many but these are manifest only in the immediate vicinity of sources. Figure 1 shows a sketch of a complex spectrum where a complex branch intersects a real branch at a ZGV point at which the slope is horizontal, i.e. where the group velocity vanishes (Mindlin, 1958a).

At any fixed frequency of excitation, there exists a finite set of real modes which —when plotted in a frequency-wavenumber diagram— show up as spectral lines that are born at the so-called *cutoff frequencies* of the system at $k = 0$ and then rise and ultimately display asymptotic trends at high frequencies. By contrast, at any fixed wavenumber there exist infinitely many characteristic frequencies. The cutoff frequencies represent plane waves of infinite wavelength which reverberate vertically up and down in the system and of which there are two types: *longitudinal* (or primary, or dilatational, or pressure, or P, or α) waves, and *transverse* (or secondary, or equivoluminal or shear, or S, or β) waves. The evaluation of the cutoff frequencies for a homogeneous system with arbitrary boundary conditions is elementary and can be written down in closed form. In the case of layered systems, a numerical solution is necessary but it can be accomplished without much ado and to any desired degree of accuracy.

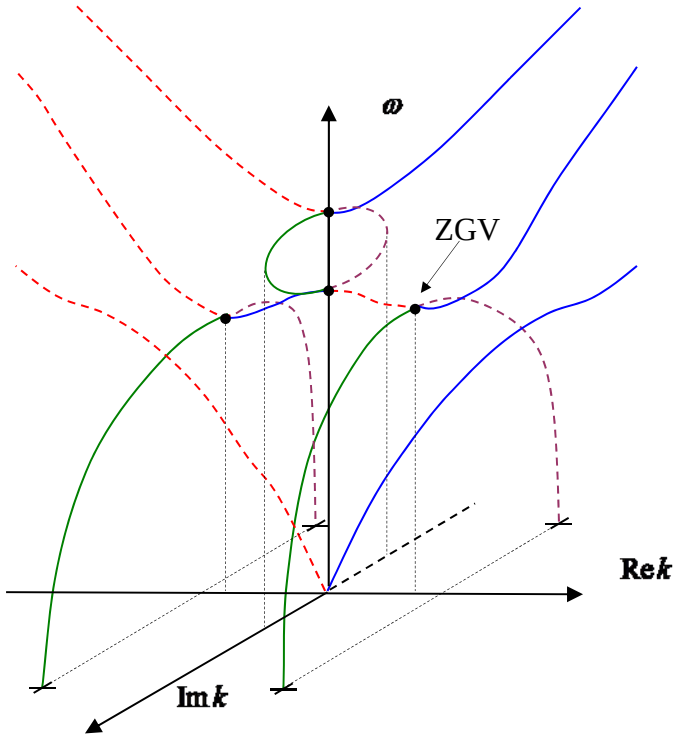

Figure 1: Complex wavenumber spectrum for a free plate (sketch after Mindlin, 1958a)

With regard to the frequency-wavenumber spectrum for an arbitrary layered medium and the location of ZGV points within that spectrum, we make in the ensuing a number of statements whose detailed proof can be found in *Appendix A*. We also defer for now the issue of the computation of an actual spectrum which is taken up in *Appendix B*. Let

$$\mathbf{u}(k,z,\omega_n)=\boldsymbol{\phi}_n(z)\mathrm{e}^{\mathrm{i}(\omega_n t-kx)} \qquad \boldsymbol{\phi}_n(z)=\begin{Bmatrix} U_n \\ -\mathrm{i}W_n \end{Bmatrix} \tag{1}$$

denote a Rayleigh-Lamb mode whose horizontal and vertical components $U_n(z), W_n(z)$ satisfy all of the boundary conditions and define the modal shape that results from the solution of an appropriate, transcendental eigenvalue problem. The characteristic frequency ω_n is the eigenvalue, $n=1,2,\cdots\infty$ is an integer modal counter, and the horizontal wavenumber k is taken as a known, real parameter. The imaginary factor in the vertical component is included herein for reasons of convenience, for it renders all algebra real.

We define the modal coefficients

$$a_{mn}=\int_0^h\left[(\lambda+2\mu)U_mU_n+\mu W_mW_n\right]dz \tag{2a}$$

$$b_{mn}=\int_0^h\left[\left(\lambda U_m\frac{dW_n}{dz}-\mu\frac{dU_m}{dz}W_n\right)+\left(\lambda\frac{dW_m}{dz}U_n-\mu W_m\frac{dU_n}{dz}\right)\right]dz \tag{2b}$$

$$g_{mn}=\int_0^h\left[\mu\frac{dU_m}{dz}\frac{dU_n}{dz}+(\lambda+2\mu)\frac{dW_m}{dz}\frac{dW_n}{dz}\right]dz \tag{2c}$$

$$m_{mn}=\int_0^h(U_mU_n+W_mW_n)\rho\,dz=\delta_{mn} \tag{2d}$$

which are all symmetric in the sub-indices (i.e. $a_{mn}=a_{nm}$ etc.). In terms of these coefficients, it is shown in *Appendix A* that the modes satisfy the following pair of *orthogonality conditions*:

$$m_{mn}=\delta_{mn}=\begin{cases}1 & m=n\\ 0 & m\neq n\end{cases} \tag{3a}$$

$$a_{mn}k^2+b_{mn}k+g_{mn}=\begin{cases}\omega_n^2 & m=n\\ 0 & m\neq n\end{cases} \tag{3b}$$

which hold true even when the material parameters change with z. Observe that in these equations we have arbitrarily normalized the modes to have unit modal mass. As also shown in *Appendix A*, a perturbation analysis to these equations yields the following derivatives with respect to the horizontal wavenumber, which we designate with primes:

$$\frac{\partial}{\partial k}\begin{Bmatrix}U_m\\ W_m\end{Bmatrix}=\begin{Bmatrix}U_m'\\ W_m'\end{Bmatrix}=\sum_{j=1}^{\infty}\begin{Bmatrix}U_m\\ W_m\end{Bmatrix}\gamma_{jm} \tag{4a}$$

$$\gamma_{mn} = \frac{2k\,a_{mn} + b_{mn}}{\omega_n^2 - \omega_m^2} \tag{4b}$$

$$\omega_n' = \frac{k\,a_{nn} + \frac{1}{2} b_{nn}}{\omega_n} = V_{gr} \quad = \text{group velocity} \tag{4c}$$

$$\omega_n'' = \frac{1}{\omega_n}\left[a_{nn} - \left(\omega_n'\right)^2 - \sum_{j=1,\, j\neq n}^{\infty} \frac{\left(2k a_{jn} + b_{jn}\right)^2}{\omega_j^2 - \omega_n^2} \right] \tag{4d}$$

In particular, any ZGV point $[k, \omega_n, \omega_n' = 0]$ satisfies the identity $k\,a_{nn} + \frac{1}{2} b_{nn} = 0$. Moreover, a ZVG point admits not only its actual eigenmode $\boldsymbol{\phi}_n(k, \omega_n, \omega_n' = 0)$, but also an *exceptional mode* of the form:

$$\mathbf{u}(k, \omega_n) = \boldsymbol{\psi}(z)\, \mathrm{e}^{\mathrm{i}(\omega_n t - kx)} = \left(\boldsymbol{\phi}_n' - \mathrm{i}\, x \boldsymbol{\phi}_n\right) \mathrm{e}^{\mathrm{i}(\omega_n t - kx)} \tag{5a}$$

which in our simpler notation translates into

$$U_{\mathrm{exc}} = U_n' - \mathrm{i}\, x U_n\,, \qquad W_{\mathrm{exc}} = W_n' - \mathrm{i}\, x W_n \tag{5b}$$

with the derivatives computed as in (4a,b). It was Mindlin (1958b) who first predicted that such exceptional modes would exist at all non-repeated cutoff frequencies. Although they appear to violate the boundedness at $x = \pm\infty$, they can arise and have been observed at the edges of plates of finite width. More recently, Tassoulas and Akylas (1984) extended Mindlin's results to all ZGV points, even those whose wavenumber is not zero, and discussed their physical implications at length. They also made references to experiments where the resonances associated with exceptional modes were clearly observed at the plate's perimeter when excited at the appropriate frequency. In *Appendix A,* we provide in turn a further generalization confirming that such exceptional modes arise at all ZGV points of an arbitrarily layered medium.

At the cutoff frequencies $k = 0$, the modes decouple into pure longitudinal α modes and transverse β modes, in which case equations (3,4) simplify further into

$$\phi_\alpha\left(k = 0, \omega_\alpha, z\right) = \begin{Bmatrix} 0 \\ W_\alpha \end{Bmatrix}, \qquad \phi_\beta\left(k = 0, \omega_\beta, z\right) = \begin{Bmatrix} U_\beta \\ 0 \end{Bmatrix} \tag{7a}$$

$$a_{\alpha\alpha} = \int_0^H \mu\, W_\alpha^2\, dz\,, \qquad m_{\alpha\alpha} = \int_0^H \rho\, W_\alpha^2\, dz = 1 \tag{7b}$$

$$a_{\beta\beta} = \int_0^H \left(\lambda + 2\mu\right) u_\beta^2\, dz \qquad m_{\beta\beta} = \int_0^H \rho\, u_\beta^2\, dz = 1 \tag{7c}$$

$$b_{\alpha\beta} = b_{\beta\alpha} = \int_0^h \left(\lambda \frac{dW_\alpha}{dz} U_\beta - \mu\, W_\alpha \frac{dU_\beta}{dz} \right) dz\,, \qquad \alpha, \beta = 1, 2, 3, \cdots \tag{7d}$$

$$\omega_\alpha'' = \frac{1}{\omega_\alpha}\left[a_{\alpha\alpha} - \sum_{\beta=1}^{\infty} \frac{b_{\beta\alpha}^2}{\omega_\beta^2 - \omega_\alpha^2} \right], \qquad \omega_\beta'' = \frac{1}{\omega_\beta}\left[a_{\beta\beta} - \sum_{\alpha=1}^{\infty} \frac{b_{\alpha\beta}^2}{\omega_\alpha^2 - \omega_\beta^2} \right] \tag{7e}$$

where the modal counters α, β now run independently and conveniently through all natural numbers; thus, they substitute for the distinct pairs (m,n) that apply to the combined set of such modes and which are needed when the modes are coupled for $k \neq 0$.

Observe that at any cutoff frequency that is not repeated, $b_{nn} = 0$ in (4c) because for $k = 0$ a horizontal mode S has no vertical P components and vice-versa. Hence, $\omega_n' = 0$ at all non-repeated cutoff frequencies, and this holds true for any boundary conditions and whether the system is layered or homogeneous. Thus, all non-repeated cutoff frequencies are by themselves ZGV modes.

Still, at least in a homogeneous plate, a coincidence of two cutoff frequencies can recur at periodic intervals whenever the wave velocity ratio $C_P / C_S = p / q$ is a rational number. Hence, at a double cutoff-frequency the group velocity is not zero, i.e. the two spectrum branches born at that point do not have a zero slope at that location, as will be shown. This was first predicted by Mindlin (1958a) and is generalized herein for an arbitrary medium. Conceivably, such a perfect coincidence of two cutoff frequencies is far less likely in either a layered plate or in an inhomogeneous plate, or at least it would not recur at regular intervals.

Now, whenever two cutoff frequencies coincide, then any linear combination of the longitudinal and transverse modes with that same frequency is also an eigenmode. For example, denote two linear combinations $\mathbf{v}_1, \mathbf{v}_2$ such as

$$\mathbf{v}_1 = \begin{Bmatrix} U_\beta \cos\theta \\ W_\alpha \sin\theta \end{Bmatrix}, \quad \mathbf{v}_2 = \begin{Bmatrix} -U_\beta \sin\theta \\ W_\alpha \cos\theta \end{Bmatrix} \tag{8}$$

where $0 \le \theta \le \frac{1}{2}\pi$ is any arbitrary angle. It can readily be shown that these two combinations are mutually orthogonal and also satisfy normality, namely equations (3a,b). In particular, for $\theta = 0$, they reduce to (7a). On the other hand, from equation (2b), we obtain for these two modes

$$b_{11} = b \sin 2\theta, \qquad b_{22} = -b \sin 2\theta \qquad b_{12} = b \cos 2\theta \tag{9a}$$

with

$$b = \int_0^h \left(\lambda U_\beta \frac{dW_\alpha}{dz} - \mu \frac{dU_\beta}{dz} W_\alpha \right) dz \tag{9b}$$

Since $b_{22} = -b_{11}$, it follows from (4c) with $k = 0$ and $\omega_1 \equiv \omega_\alpha = \omega_\beta \equiv \omega_2$ that $\omega_1' = \frac{1}{2} b_{11} / \omega_1$ and $\omega_2' = -\frac{1}{2} b_{11} / \omega_1$, with the average slope being zero. Thus, at any repeated cutoff frequency where two branches are born, one of these has positive slope and the other has an equal but negative slope i.e. a negative group velocity. The implication is that the branch with negative slope gives rise to a an anomalous spectral segment that at some point will reach a minimum and thus terminate at a ZGV mode with $k \neq 0$. Hence, we are led to the conclusion that all repeated cutoff frequencies give rise to anomalous branches

terminating at a ZGV point, even if the double cutoff frequency point itself is not one of these. However, it should also be observed that as the frequency of the double cutoff frequency increases, the magnitude of the negative slope decreases steadily in tandem with that frequency, i.e. with the modal number. Thus, double roots with very high modal number produce ZGVs which are either very close to the frequency axis or which lie only slightly below that frequency, to the point that they are virtually indistinguishable from the double root, and thus difficult to detect. Another way of saying this is that the branch exhibits an initial flat segment where the group velocity is very low.

Number of ZGV Modes

So how many ZGV modes other than those at the cutoff frequencies already referred to exist? The short answer is "very few", as will be seen. Inasmuch as a ZGV point lies in a trough of the spectral line in question and that such a line is born at a cutoff frequency, it follows that that spectral line must have a local maximum at $k = 0$. In other words, the first derivative at a non-repeated cutoff frequency is zero while the second derivative must be negative for a ZGV branch to develop. Thus, in principle all we must do to decide which branches contain ZGV modes is to apply the formulas above and test for the presence and number of negative second derivatives at $k = 0$. This number would then have to be augmented by consideration of the existence of double roots, if any.

In principle, the summations in (7e) involve infinitely many terms, which we simulate herein with N =100,000 of these, but final results were not sensitive to this number. Presumably, the accuracy of these summations could have been refined further by establishing the asymptotic trends of the summands and evaluating the tails by means of formulas such as the polygamma function. Still, using the simple and direct summation we achieved results that were quite acceptable, at least for the purposes of this article.

In the ensuing, we apply these concepts to homogeneous plates with various boundary conditions and disregard —at least for now— the possibility of repeated cutoff frequencies by assuming that the ω_α and ω_β frequencies are distinct. Also, we omit in our analyses the zero cutoff frequencies that correspond to rigid body modes in free plates, because as can be seen from (7d), the coefficient $b_{\alpha 0} = 0, b_{0\beta} = 0$, inasmuch as the rigid body mode has no vertical derivative. We also make use of the following symbols, equivalences and definitions:

$$a^2 = \frac{\mu}{\lambda + 2\mu} = \frac{\frac{1}{2} - \nu}{1 - \nu}, \qquad 1 - 2a^2 = \frac{\lambda}{\lambda + 2\mu} = \frac{\nu}{1 - \nu} \tag{10a}$$

$$a = \frac{C_S}{C_P} = \sqrt{\frac{\frac{1}{2} - \nu}{1 - \nu}}, \qquad \nu = \frac{\frac{1}{2} - a^2}{1 - a^2} \tag{10b}$$

Plate with mixed boundary conditions

A homogeneous plate endowed with any combination of *mixed* boundary conditions (i.e. "rollers") on both sides has *no* ZVG modes other than at the cutoff frequencies. The modal frequencies in such plates for any wavenumber can be found in closed form (e.g. Kausel, 2006, pp. 90-96):

Boundary conditions FC-FC, CF-CF:

$$\omega_\alpha = \frac{C_P}{H}\sqrt{\kappa^2 + \pi^2\alpha^2}, \quad \kappa = kh, \qquad \alpha = 1,2,3,\cdots \tag{11a}$$

$$\omega_\beta = \frac{C_S}{H}\sqrt{\kappa^2 + \pi^2\beta^2} \qquad \beta = 1,2,3,\cdots \tag{11b}$$

Boundary conditions FC-CF, CF-FC:

$$\omega_\alpha = \frac{C_P}{H}\sqrt{\kappa^2 + \pi^2\left(\alpha - \tfrac{1}{2}\right)^2} \tag{12a}$$

$$\omega_\beta = \frac{C_S}{H}\sqrt{\kappa^2 + \pi^2\left(\beta - \tfrac{1}{2}\right)^2} \tag{12b}$$

In 11a-12b, the cutoff frequencies follow by setting $\kappa = 0$

Plate with boundary conditions FF-FC or FF-CF

This case need not be considered separately herein because its modes agree with either the symmetric or the anti-symmetric modes of a homogeneous, free plate of double thickness.

Homogeneous stratum:

In the case of a homogeneous stratum (FF-CC), the P and S modal parameters are

$$\omega_\alpha = \frac{\pi C_P}{h}\left(\alpha - \tfrac{1}{2}\right), \qquad w_\alpha(z) = \sqrt{\tfrac{2}{\rho h}}\cos\left[\pi\left(\alpha - \tfrac{1}{2}\right)\zeta\right], \qquad \zeta = z/h$$

$$\omega_\beta = \frac{\pi C_S}{h}\left(\beta - \tfrac{1}{2}\right), \qquad u_\beta(z) = \sqrt{\tfrac{2}{\rho h}}\cos\left[\pi\left(\beta - \tfrac{1}{2}\right)\zeta\right]$$

$$a_{\alpha\alpha} = C_S^2 = a^2 C_P^2 \qquad a_{\beta\beta} = C_P^2$$

$$\frac{b_{\alpha\beta}^2}{\omega_\alpha^2 - \omega_\beta^2} = \left(\frac{2}{\pi}\right)^2 \frac{\left[\left(1-2a^2\right)\left(\alpha - \tfrac{1}{2}\right)I_{\alpha\beta} - a^2\left(\beta - \tfrac{1}{2}\right)I_{\beta\alpha}\right]^2}{\left(\alpha - \tfrac{1}{2}\right)^2 - a^2\left(\beta - \tfrac{1}{2}\right)^2} C_P^2$$

$$I_{\alpha\beta} = \pi\int_0^1 \sin\pi\left(\alpha - \tfrac{1}{2}\right)\zeta \;\cos\pi\left(\beta - \tfrac{1}{2}\right)\zeta \; d\zeta = \begin{cases} (\alpha+\beta-1)^{-1} & \alpha+\beta \text{ is even} \\ (\beta-\alpha)^{-1} & \alpha+\beta \text{ is odd} \end{cases}$$

(13a-e)

Homogeneous plate:

In the case of a homogeneous plate (FF-FF), the P and S modal parameters are

$$\omega_\alpha = \frac{\pi C_P}{h}\alpha, \qquad w_\alpha(z) = \sqrt{\tfrac{2}{\rho h}}\cos(\pi\alpha\zeta), \quad \alpha = 1,2,3,\cdots \quad \zeta = z/h$$

$$\omega_\beta = \frac{\pi C_S}{h}\beta, \qquad u_\beta(z) = \sqrt{\tfrac{2}{\rho h}}\cos(\pi\beta\zeta), \quad \beta = 1,2,3,\cdots$$

$$a_{\alpha\alpha} = C_S^2, \qquad a_{\beta\beta} = C_P^2$$

$$\frac{b_{\alpha\beta}^2}{\omega_\alpha^2 - \omega_\beta^2} = \left(\frac{2}{\pi}\right)^2 \frac{\left[\left(1-2a^2\right)J_{\alpha\beta} - a^2 J_{\beta\alpha}\right]^2}{\alpha^2 - a^2\beta^2} C_P^2$$

$$J_{\alpha\beta} = \pi\alpha \int_0^1 \sin \pi\alpha\zeta \ \cos \pi\beta\zeta \ d\zeta = \begin{cases} 0 & \alpha+\beta \text{ is even} \\ 2\dfrac{\alpha^2}{\alpha^2-\beta^2} & \alpha+\beta \text{ is odd} \end{cases}$$

(14a-e)

By and large, we found only a handful of ZGV modes of very low modal order which were followed by a highly rarified region containing just a few isolated points of high modal order. Most of those modes were of the S type and a minority of the P type. Furthermore, we found that the number of ZGV poles decreases with Poisson's ratio after a value of about 0.25, and especially after $\nu = 0.40$. Tables 1 and 2 provide a summary of ZGV branches found for a uniform plate and a uniform stratum, respectively. We applied the preceding exact formulas and searched for negative second derivatives among the first *five hundred* P modes and an equal number of S modes in both a stratum and in a plate of various Poisson's ratios. We then repeated the search using the Thin-Layer Method (TLM) [9-12] described briefly in *Appendix B*, a discrete formulation based on the finite element method which not only provided comparable results but also the dispersion spectra for either homogeneous or layered media. A question mark in the tables after the last modal number indicates uncertainties due to numerical error, in most cases because the magnitude of the second derivative was very small. By contrast, a dash means that we found no further ZGV branches up to the 500 limit with either technique.

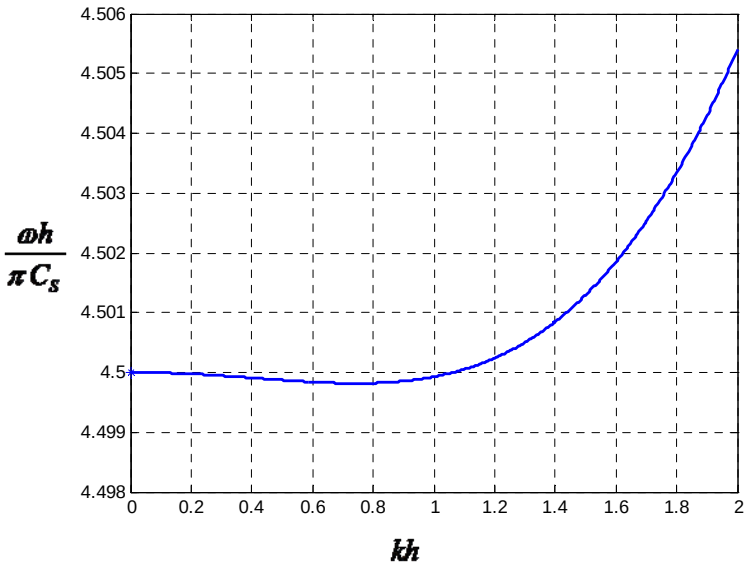

Figure 2: S_5 branch for $\nu = 0.$, homogeneous stratum

In general, it was difficult to confirm the reality of negative second derivatives beyond, say, the 50th P mode, because the magnitude of those derivatives was very small and thus rather prone to round-off errors. In addition the branches of high modes associated with ZGVs were rather flat near the frequency axis. Figure 2, which shows the fifth S mode in a stratum with $\nu = 0.$, illustrates this point: Although the ZGV point can still be clearly discerned, this is so only after some massive magnification, as can be verified by observing the scale used for the frequency axis. Sharp-eye readers may also have noticed

that we omitted $\nu = 0.10$ for the plate –but not for the stratum– because that value leads to a wave speed ratio $C_P / C_S = \frac{3}{2}$, which results in a large number of coincident cutoff frequencies in the plate, and thus of ZGV modes. As can be seen, even the small change in Poisson's ratio from 0.10 to 0.11 leads to an abrupt fall in the number of ZGV modes, because the speed ratio is no longer a rational number.

Table 1: Homogeneous plate:

ν	C_S / C_P	**Type**	**Mode number**					
0	0.707	S	4	24	140?			
		P	1	2	7	12	41	70?
0.11	0.662	S	3	4	9	15	21	74?
		P	1	–				
0.15	0.642	S	3	4	14	42?		
		P	1	34	77	274?		
0.20	0.612	S	3	8	13	80?		
		P	1	11	30	109?		
0.25	0.577	S	3	12	45	168?		
		P	1	4	15	56?		
0.30	0.535	S	3	11	28	101?		
		P	1	8	31	240?		
0.35	0.480	S	2	6	52	102?		
		P	12	–				
0.40	0.408	S	2	12	22	120?		
		P	2	20	198?			
0.45	0.302	S	2	–				
		P	–					

Table 2: Homogeneous stratum:

ν	C_S / C_P	**Type**	**Mode number**				
0	0.707	S	4	5	11	45	120?
		P	2	27	56?		
0.10	0.667	S	4	10	–		
		P	2	–			
0.15	0.642	S	4	9	48	154?	
		P	2	13	56?		
0.20	0.612	S	4	29	65?		
		P	1	2	21	–	
0.25	0.577	S	3	8	36	107?	
		P	1	10	133?		
0.30	0.535	S	3	7	20	80?	
		P	1	20	–		
0.35	0.480	S	3	14	141?		
		P	1	31?			
0.40	0.408	S	3	6	9	36	303?
		P	1	55?			
0.45	0.302	S	2	5	22	32	231?
		P	–				

Finally, Figure 3 shows the spectrum for a layered plate, with stars and circles indicating the cutoff frequencies for S and P modes, respectively. The free plate had the following properties:

Table 3: Layered, free plate

Layer	Mass Density	Thickness	Shear modulus	Sh. wave velocity	Poisson's ratio
1	1.00	0.25	1.0000	1.00	0.00
2	1.00	0.50	1.5625	1.25	0.05
3	1.00	0.25	1.2100	1.10	0.11

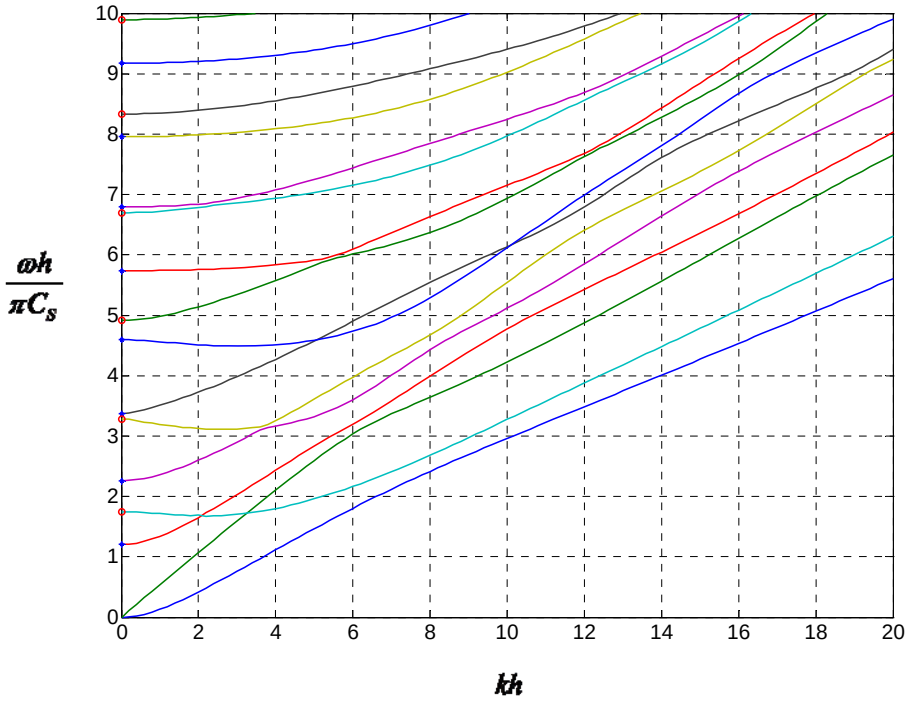

Figure 3: Wavenumber spectrum for layered plate

This time only a numerical solution via the TLM (with 200 quadratic thin layers) was possible, see *Appendix B*. That model predicted that the S modes 4,16,29,48, 110, … and the P modes 1,2,89 … would sustain ZGV modes.

In summary, although it may well be that infinitely many ZGV modes exist in a homogeneous stratum or plate —especially if cutoff frequencies are repeated— for practical purposes their number is in the single digits, at least in the range of engineering interest, inasmuch as for the most part only some five or so S and P branches of low modal order are clearly manifest.

Locating the ZGV modes

How can the actual ZGV points be located without searching for their presence in a complete wavenumber spectrum, indeed, without computing any other modal branches?

The strategy is simple: Start at a cutoff frequency at which the second derivative is negative –or where a double cutoff frequency exists– and march forward from there along that branch, evaluating the path in small increments. In the TLM approach (*Appendix B*), this could be accomplished in the context of an inverse iteration scheme with shift by the Rayleigh quotient, computing not only the projected eigenvalue —i.e. the next point on the branch— but also its first derivative via eq. 4c, and using both to estimate the neighboring point lying ahead on that branch. Also, the second derivative could be obtained as a by-product in the context of a backward difference scheme —the formula in (4d) is not applicable because only one (i.e. the current) mode will be available once $k > 0$.

Conclusions

In this paper, we considered the problem of how many zero group velocity (ZVG) modes exist in an inhomogeneous plate at points other than those at cutoff frequencies, and also how these can readily be located. The following findings apply to any arbitrary layered plate and with any combination of boundary conditions:

- The group velocity vanishes at all non-repeated cutoff frequencies. This fact had already been established by Mindlin (1958b) in the context of a homogeneous plate.
- Each and every ZGV point admits an additional *exceptional* mode that varies linearly in the direction of wave propagation, and which may lead to edge resonances in plates of finite width. Such modes exist not only at the cutoff frequencies, but also at all ZGV points (Tassoulas and Akylas, 1984). We have further shown that this is also true in layered plates with arbitrary boundary conditions.
- In a homogeneous plate where the ratio of longitudinal to transverse wave speed is a rational number, repeated cutoff frequencies can arise at which two branches with opposite slope will be born. The descending branch will necessarily give rise to a ZVG with a non-zero wavenumber. Still, such repeated cutoff frequencies are much less likely in a layered plate or an inhomogeneous plate.
- Whenever cutoff frequencies are repeated at periodic intervals, there exist infinitely many ZVG's. However, high order ZVG's —whether or not any cutoff frequencies are repeated— lie in branches that are so flat that for practical purposes they do not materialize, and presumably any attenuation will wipe them out as well. Thus, for practical purposes, only a handful of low order modes is capable of sustaining ZVG modes of engineering interest.
- Whenever the cutoff frequencies are not repeated, the number of ZGV modes with non-zero wavenumber is rather small, numbering in the single digits. For the most part they are of the S type, and appear in branches of low modal order.
- ZGV's can be located by starting at a cutoff frequency with negative second derivative, or following the descending branch of a double cutoff frequency.
- The number of ZVG's decreases with Poisson's ratio. This is mainly the result of the growing separation of the cutoff frequencies of P modes from those of the S modes as Poisson's ratio increases.

Appendix A

Rayleigh-Lamb modes in a layered medium

Consider a horizontally homogeneous, elastic medium of finite thickness h characterized by a depth-dependent shear modulus $\mu(z)$, Lamé constant $\lambda(z)$ and mass density $\rho(z)$. With appropriate use of singularity functions, this description also can be made to include layered media for which the properties are locally homogeneous while changing abruptly from layer to layer. Also, the boundary conditions at either surface are arbitrary. In the absence of body forces, the displacement field must satisfy the elastic wave equations for vertically inhomogeneous media in plane strain

$$\rho\frac{\partial^2 u}{\partial t^2}-(\lambda+2\mu)\frac{\partial^2 u}{\partial x^2}-\frac{\partial}{\partial z}\left(\mu\frac{\partial u}{\partial z}\right)-\frac{\partial}{\partial x}\left(\lambda\frac{\partial w}{\partial z}+\frac{\partial(\mu w)}{\partial z}\right)=0 \qquad \text{(A1a)}$$

$$\rho\frac{\partial^2 w}{\partial t^2}-\mu\frac{\partial^2 w}{\partial x^2}-\frac{\partial}{\partial z}\left((\lambda+2\mu)\frac{\partial w}{\partial z}\right)-\frac{\partial}{\partial x}\left(\mu\frac{\partial u}{\partial z}+\frac{\partial(\lambda u)}{\partial z}\right)=0 \qquad \text{(A1b)}$$

together with some appropriate boundary conditions at the top and bottom surface, the details of which are of no particular concern to us here. Assume next that such medium admits free Rayleigh-Lamb waves which can be written as

$$u(x,z,t)=U_n(k,z)e^{\mathrm{i}(\omega_n t-kx)} \qquad \text{(A2a)}$$

$$w(x,z,t)=-\mathrm{i}W_n(k,z)e^{\mathrm{i}(\omega_n t-kx)} \qquad \text{(A2b)}$$

in which the mode satisfies all of the boundary conditions and defines the modal shape that results from the solution of an appropriate, transcendental eigenvalue problem. The characteristic frequency ω_n is the eigenvalue, n is an integer modal index or modal counter, and the horizontal wavenumber k is taken as a known, real parameter. The imaginary factor in the vertical component is included for reasons of convenience for it renders all algebra real. To be admissible, the ansatz (A2) must satisfy the Fourier-transformed dynamic equilibrium equations

$$k^2(\lambda+2\mu)U_n+k\left(\lambda\frac{dW_n}{dz}+\frac{d}{dz}(\mu W_n)\right)-\frac{d}{dz}\left(\mu\frac{dU_n}{dz}\right)-\rho\omega_n^2U_n=0 \qquad \text{(A3a)}$$

$$k^2\mu W_n-k\left(\mu\frac{dU_n}{dz}+\frac{d}{dz}(\lambda U_n)\right)-\frac{d}{dz}\left((\lambda+2\mu)\frac{dW_n}{dz}\right)-\rho\omega_n^2W_n=0 \qquad \text{(A3b)}$$

Orthogonality:

Consider next a distinct mode $[k,\omega_m,U_m,W_m]$, multiply eq. (A2a) by U_m and (A2b) by W_m and add these two equations, then integrate the result over the thickness. Integrating again by parts and taking into account whatever boundary conditions may apply, we obtain

$$k^2\int_0^h\left[(\lambda+2\mu)U_mU_n+\mu W_mW_n\right]dz+k\int_0^h\left[\lambda\left(U_m\frac{dW_n}{dz}+U_n\frac{dW_m}{dz}\right)-\mu\left(W_m\frac{dU_n}{dz}+W_n\frac{dU_m}{dz}\right)\right]dz$$
$$+\int_0^h\left[\mu\frac{dU_m}{dz}\frac{dU_n}{dz}+(\lambda+2\mu)\frac{dW_m}{dz}\frac{dW_n}{dz}\right]dz-\omega_n^2\int_0^h\rho\left(U_mU_n+W_mW_n\right)dz=0 \tag{A4}$$

Interchanging the indices m,n and subtracting the resulting expression from one another, we obtain

$$\left(\omega_m^2-\omega_n^2\right)\int_0^h\rho\left(U_mU_n+W_mW_n\right)dz=0 \tag{A5}$$

which leads immediately to the *first orthogonality condition*

$$\int_0^h\left(U_mU_n+W_mW_n\right)\rho\,dz=\delta_{mn}=\begin{cases}1 & m=n\\ 0 & m\neq n\end{cases} \tag{A6}$$

where we have chosen to scale the eigenvectors so that they have a unit modal mass. Eqs. (A4) and (A6) imply in turn the *second orthogonality condition*

$$k^2\int_0^h\left[(\lambda+2\mu)U_mU_n+\mu W_mW_n\right]dz+k\int_0^h\left[\lambda\left(U_m\frac{dW_n}{dz}+U_n\frac{dW_m}{dz}\right)-\mu\left(W_m\frac{dU_n}{dz}+W_n\frac{dU_m}{dz}\right)\right]dz$$
$$+\int_0^h\left[\mu\frac{dU_m}{dz}\frac{dU_n}{dz}+(\lambda+2\mu)\frac{dW_m}{dz}\frac{dW_n}{dz}\right]dz=\delta_{mn}\omega_n^2=\begin{cases}\omega_n^2 & m=n\\ 0 & m\neq n\end{cases} \tag{A7}$$

We define the coefficients

$$\begin{aligned}
a_{mn}&=\int_0^h\left[(\lambda+2\mu)U_mU_n+\mu W_mW_n\right]dz\\
b_{mn}&=\int_0^h\left[\left(\lambda U_m\frac{dW_n}{dz}-\mu W_m\frac{dU_n}{dz}\right)+\left(\lambda\frac{dW_m}{dz}U_n-\mu\frac{dU_m}{dz}W_n\right)\right]dz\\
g_{mn}&=\int_0^h\left[\mu\frac{dU_m}{dz}\frac{dU_n}{dz}+(\lambda+2\mu)\frac{dW_m}{dz}\frac{dW_n}{dz}\right]dz\\
m_{mn}&=\int_0^h\left(U_mU_n+W_mW_n\right)\rho\,dz=\delta_{mn}
\end{aligned} \tag{A8}$$

which are symmetric in m,n (i.e. $a_{mn}=a_{nm}$ etc.). In terms of these coefficients, eq. A7 can be written in compact form as

$$a_{mn}k^2+b_{mn}k+g_{mn}=\omega_n^2\delta_{mn} \tag{A9}$$

It should be noticed that all of these expressions and properties apply no matter how the material properties change with depth and whatever the boundary conditions.

Derivatives with respect to wavenumber:

Consider next the derivative of eq. (A6) with respect to the horizontal wavenumber, which we designate with single primes:

$$\int_0^h \left(U'_m U_n + W'_m W_n + U_m U'_n + W_m W'_n\right)\rho\, dz = 0 \tag{A10}$$

Expressing the modal derivatives in terms of the modes with modal coordinates γ_{jm}, i.e.

$$\boldsymbol{\phi}'_m = \sum_{j=1}^{\infty} \boldsymbol{\phi}_j \gamma_{jm} \qquad \text{or} \qquad \begin{Bmatrix} U'_m \\ W'_m \end{Bmatrix} = \sum_{j=1}^{\infty} \begin{Bmatrix} U_m \\ W_m \end{Bmatrix} \gamma_{jm} \tag{A11}$$

we obtain

$$\sum_{j=1}^{\infty} \int_0^h \left(\left(U_j U_n + W_j W_n\right)\gamma_{jm} + \left(U_m U_j + W_m W_j\right)\gamma_{jn}\right)\rho\, dz = 0 \tag{A12}$$

and because of the first orthogonality condition, this reduces to

$$\sum_{j=1}^{\infty} \left(\delta_{jn}\gamma_{jm} + \delta_{jm}\gamma_{jn}\right) = 0 \tag{A13a}$$

or

$$\gamma_{nm} + \gamma_{mn} = 0 \tag{A13b}$$

so

$$\gamma_{nn} = 0, \qquad \gamma_{nm} = -\gamma_{mn} \tag{A14}$$

In a similar fashion we can also write down without much ado the derivatives of the coefficients (A8), which are:

$$\begin{aligned} a'_{mn} &= \sum_{j=1}^{\infty} \left(a_{jn}\gamma_{jm} + a_{jm}\gamma_{jn}\right), & a'_{nn} &= 2\sum_{j=1}^{\infty} a_{jn}\gamma_{jn} \\ b'_{mn} &= \sum_{j=1}^{\infty} \left(b_{jn}\gamma_{jm} + b_{jm}\gamma_{jn}\right) & b'_{nn} &= 2\sum_{j=1}^{\infty} b_{jn}\gamma_{jn} \\ g'_{mn} &= \sum_{j=1}^{\infty} \left(g_{jn}\gamma_{jm} + g_{jm}\gamma_{jn}\right) & m'_{mn} &= 0 \end{aligned} \tag{A15}$$

Hence, the derivative of eq. (A9) is

$$2a_{mn}k + b_{mn} - 2\omega_n\omega'_n\delta_{mn} + \sum_{j=1}^{\infty}\left(a_{jm}k^2 + b_{jm}k + g_{jm}\right)\gamma_{jn} + \sum_{j=1}^{\infty}\left(a_{jn}k^2 + b_{jn}k + g_{jn}\right)\gamma_{jm} = 0 \tag{A16}$$

Now, since each term in the summations satisfies equation A9, then

$$2a_{mn}k + b_{mn} - 2\omega_n\omega'_n\,\delta_{mn} + \omega_m^2\gamma_{mn} + \omega_n^2\gamma_{nm} = 0 \tag{A17}$$

and with eq. (A14)

$$2a_{mn}k + b_{mn} + \gamma_{mn}\left(\omega_m^2 - \omega_n^2\right) = \delta_{mn}\, 2\omega_n\omega_n' \tag{A18a}$$

$$2a_{nn}k + b_{nn} = 2\omega_n\omega_n' \tag{A18b}$$

so

$$\boxed{\gamma_{mn} = \frac{2k\, a_{mn} + b_{mn}}{\omega_n^2 - \omega_m^2}}, \qquad m \neq n \qquad \text{and} \qquad \boxed{\omega_n' = \frac{k\, a_{nn} + \frac{1}{2} b_{nn}}{\omega_n}} \tag{A19}$$

At any cutoff frequency that is not repeated, $b_{nn} = 0$ because for $k = 0$, a horizontal mode S has no vertical P components and vice-versa. Hence, $\omega_n' = 0$ at all non-repeated cutoff frequencies, and this is true for any boundary conditions and whether the system is layered or homogeneous. Thus, all non-repeated cutoff frequencies are ZGV modes.
Consider next the derivative of (A18b):

$$a_{nn} + ka_{nn}' + \tfrac{1}{2} b_{nn}' = \omega_n\omega_n'' + \left(\omega_n'\right)^2 \tag{A20}$$

or

$$a_{nn} + 2k\sum_{j=1}^{\infty} a_{jn}\gamma_{jn} + \sum_{j=1}^{\infty} b_{jn}\gamma_{jn} = \omega_n\omega_n'' + \left(\omega_n'\right)^2 \tag{A21}$$

In particular, at all non-repeated cutoff frequencies and using (A19)

$$\boxed{\omega_n'' = \frac{1}{\omega_n}\left[a_{nn} - \sum_{j=1,\, j\neq n}^{\infty} \frac{b_{jn}^2}{\omega_j^2 - \omega_n^2}\right]}, \qquad k = 0\,,\ \omega_n' = 0 \tag{A22}$$

Exceptional modes

Consider next the variation with the horizontal wavenumber of the contribution of a single mode to the displacement vector at a ZGV location in the spectrum, i.e. a point where $\omega_n' = 0$:

$$\frac{\partial \mathbf{u}(k, \omega_n)}{\partial k} = \frac{\partial}{\partial k}\left(\boldsymbol{\phi}_n \mathrm{e}^{\mathrm{i}(\omega_n t - kx)}\right) = \left(\boldsymbol{\phi}_n' - \mathrm{i}\, x\boldsymbol{\phi}_n\right)\mathrm{e}^{\mathrm{i}(\omega_n t - kx)} = \boldsymbol{\psi}(z)\,\mathrm{e}^{\mathrm{i}(\omega_n t - kx)} \tag{A23a}$$

$$\boldsymbol{\phi}_n = \begin{Bmatrix} U_n \\ -\mathrm{i}W_n \end{Bmatrix} \tag{A23b}$$

whose spatial-x derivatives are

$$\frac{\partial}{\partial x}\left[\boldsymbol{\psi}(z)\,\mathrm{e}^{\mathrm{i}(\omega_n t - kx)}\right] = -\mathrm{i}\left(k\boldsymbol{\psi} + \boldsymbol{\phi}_n\right)\mathrm{e}^{\mathrm{i}(\omega_n t - kx)} \tag{A24a}$$

$$\frac{\partial^2}{\partial x^2}\left[\boldsymbol{\psi}(z)\,\mathrm{e}^{\mathrm{i}(\omega_n t - kx)}\right] = -\left(k^2\boldsymbol{\psi} + 2k\boldsymbol{\phi}_n\right)\mathrm{e}^{\mathrm{i}(\omega_n t - kx)} \tag{A24b}$$

Following Tassoulas and Akylas, we now claim that $\boldsymbol{\psi}(z)=\boldsymbol{\phi}_n'-\mathrm{i}\,x\boldsymbol{\phi}_n$ is an *exceptional mode* at points of ZGV, including those at which the wavenumber is not zero. To demonstrate this, we begin by substituting (A23, A34) into equations (A1), and after brief algebra we obtain

$$\begin{aligned}
&+2k(\lambda+2\mu)U_n+\left(\lambda\frac{\partial W_n}{\partial z}+\frac{\partial(\mu W_n)}{\partial z}\right)\\
&\left[k^2(\lambda+2\mu)-\rho\omega_n^2\right]U_n'+k\left(\lambda\frac{\partial W_n'}{\partial z}+\frac{\partial(\mu W_n')}{\partial z}\right)-\frac{\partial}{\partial z}\left(\mu\frac{\partial uU_n'}{\partial z}\right)\\
&-\mathrm{i}\,x\left[\left(k^2(\lambda+2\mu)-\rho\omega_n^2\right)U_n+k\left(\lambda\frac{\partial W_n}{\partial z}+\frac{\partial(\mu W_n)}{\partial z}\right)-\frac{\partial}{\partial z}\left(\mu\frac{\partial U_n}{\partial z}\right)\right]=0
\end{aligned}\tag{A25a}$$

and

$$\begin{aligned}
&2\mu kW_n-\left(\mu\frac{\partial U_n}{\partial z}+\frac{\partial(\lambda U_n)}{\partial z}\right)\\
&-\mathrm{i}\,x\left[\left(k^2\mu-\rho\omega_n^2\right)W_n-k\left(\mu\frac{\partial U_n}{\partial z}+\frac{\partial(\lambda U_n)}{\partial z}\right)-\frac{\partial}{\partial z}\left((\lambda+2\mu)\frac{\partial W_n}{\partial z}\right)\right]\\
&+\left(\mu k^2-\rho\omega_n^2\right)W_n'-k\left(\mu\frac{\partial U_n'}{\partial z}+\frac{\partial(\lambda U_n')}{\partial z}\right)-\frac{\partial}{\partial z}\left((\lambda+2\mu)\frac{\partial W_n'}{\partial z}\right)=0
\end{aligned}\tag{A25b}$$

Now, the terms in brackets multiplied by $\mathrm{i}\,x$ are the equations (A2) for the n^{th} mode, so they vanish identically. Hence

$$\begin{aligned}
&2k(\lambda+2\mu)U_n+\left(\lambda\frac{\partial W_n}{\partial z}+\frac{\partial(\mu W_n)}{\partial z}\right)\\
&+\left\{k^2(\lambda+2\mu)U_n'+k\left(\lambda\frac{\partial W_n'}{\partial z}+\frac{\partial(\mu W_n')}{\partial z}\right)-\frac{\partial}{\partial z}\left(\mu\frac{\partial uU_n'}{\partial z}\right)-\rho\omega_n^2U_n'\right\}=0
\end{aligned}\tag{A26a}$$

$$\begin{aligned}
&2\mu kW_n-\left(\mu\frac{\partial U_n}{\partial z}+\frac{\partial(\lambda U_n)}{\partial z}\right)\\
&+\left\{k^2\mu W_n'-k\left(\mu\frac{\partial U_n'}{\partial z}+\frac{\partial(\lambda U_n')}{\partial z}\right)-\frac{\partial}{\partial z}\left((\lambda+2\mu)\frac{\partial W_n'}{\partial z}\right)-\rho\omega_n^2W_n'\right\}=0
\end{aligned}\tag{A26b}$$

On the other hand, taking the derivative of eqs. A2 with respect to k, we obtain

$$\begin{aligned}
&2k(\lambda+2\mu)U_n+\left(\lambda\frac{dW_n}{dz}+\frac{d}{dz}(\mu W_n)\right)-2\rho\,\omega_n\omega_n'U_n\\
&+\left\{k^2(\lambda+2\mu)U_n'+k\left(\lambda\frac{dW_n'}{dz}+\frac{d}{dz}(\mu W_n')\right)-\frac{d}{dz}\left(\mu\frac{dU_n'}{dz}\right)-\rho\,\omega_n^2U_n'\right\}=0
\end{aligned}\tag{A27a}$$

and

$$2k\mu W_n - \left(\mu\frac{dU_n}{dz} + \frac{d}{dz}\left(\lambda U_n\right)\right) - 2\rho\omega_n\omega_n' W_n$$
$$+\left\{k^2\mu W_n' - k\left(\mu\frac{dU_n'}{dz} + \frac{d}{dz}\left(\lambda U_n'\right)\right) + \frac{d}{dz}\left(\left(\lambda+2\mu\right)\frac{dW_n'}{dz}\right) - \rho\omega_n^2 W_n'\right\} = 0 \qquad \text{(A27b)}$$

Comparison of (A26a,b) with (A27a,b) indicates that they agree perfectly provided that $\omega_n' = 0$, i.e. that the point is a ZGV point. We rush to add, however, that although the exceptional mode does satisfy the equations of motion at ZGV points and thus represents a resonant condition of the medium at that wavenumber and frequency, by itself the derivative of the ZGV mode is not a mode in the sense that the terms in braces in eqs. (A26a,b) do not vanish. Tassoulas and Akylas discuss the exceptional modes at length and make references to experiments where such modes have been clearly observed.

Appendix B:

Thin Layer Method (TLM)

A most convenient tool to obtain the Rayleigh-Lamb spectrum for any horizontal wavenumber k is what is now referred to as the *thin-layer method* (TLM), which employs a finite element formulation in the direction of depth (i.e. layering), yet a continuous solution in the horizontal, unbounded direction [9-12]. In the TLM, the layered system is characterized by an algebraic, secular equation of the form (Waas [9], 1972),

$$\left(\mathbf{A}k^2 + \mathrm{i}\,\hat{\mathbf{B}}k + \mathbf{G} - \omega^2\mathbf{M}\right)\mathbf{v} = \mathbf{0} \qquad \text{(B1)}$$

in which $\mathrm{i} = \sqrt{-1}$, and all matrices are real, narrow-banded and block-tridiagonal which depend solely on the material properties, the order of the FE expansion, and the thickness of the thin layers. With the exception of $\hat{\mathbf{B}}$ that is anti-symmetric, all other matrices are symmetric, $\mathbf{A},\mathbf{M}$ are both positive definite, and $\mathbf{G}$ is positive semi-definite (definite, if the system does not allow rigid body modes). By a simple similarity transformation involving the substitution $\boldsymbol{\phi} = \mathbf{T}\mathbf{v}$ with a diagonal matrix $\mathbf{T} = diag\left(1,-\mathrm{i},1,-\mathrm{i},\cdots\right)$, it can be shown that $\mathbf{B} = \mathrm{i}\mathbf{T}\hat{\mathbf{B}}\mathbf{T}$ becomes real and symmetric, the transformation does not affect any of the other matrices, and equation (B1) simplifies into the fully real and symmetric form

$$\left(\mathbf{A}k^2 + \mathbf{B}k + \mathbf{G} - \omega^2\mathbf{M}\right)\boldsymbol{\phi} = \mathbf{0} \qquad \text{(B2)}$$

This leads to a standard real and symmetric eigenvalue problem (EVP) for Lamb waves of the form

$$\mathbf{K}\boldsymbol{\phi}_j = \omega_j^2\mathbf{M}\boldsymbol{\phi}_j, \qquad \mathbf{K}\left(k\right) = \mathbf{A}k^2 + \mathbf{B}k + \mathbf{G} \qquad \text{(B3)}$$

which can readily and effectively be solved with modern tools, say those in Matlab, even when hundreds or thousands of thin layers are used, and for any boundary conditions. The cutoff frequencies are obtained by setting $k=0$, in which case the modal components uncouple into transverse S-modes and longitudinal P-modes.

Perturbation analysis

We now proceed to write down perturbation formulas obtained by taking the first and second derivatives of eq. (B3) with respect to wavenumber, which we designate by means of single and double primes. The result is

$$\left(\mathbf{K}' - 2\omega_j\omega_j'\mathbf{M}\right)\boldsymbol{\phi}_j + \left(\mathbf{K} - \omega_j^2\mathbf{M}\right)\boldsymbol{\phi}_j' = \mathbf{0} \tag{B4a}$$

$$\left(\mathbf{K}'' - 2\left(\omega_j'^2 + \omega_j\omega_j''\right)\mathbf{M}\right)\boldsymbol{\phi}_j + 2\left(\mathbf{K}' - 2\omega_j\omega_j'\mathbf{M}\right)\boldsymbol{\phi}_j' + \left(\mathbf{K} - \omega_j^2\mathbf{M}\right)\boldsymbol{\phi}_j'' = \mathbf{0} \tag{B4b}$$

where $\mathbf{K}' = 2\mathbf{A}k + \mathbf{B}$, $\mathbf{K}'' = 2\mathbf{A}$. Expanding the vector derivatives as $\boldsymbol{\phi}_j' = \boldsymbol{\Phi}\Gamma_j = \sum \boldsymbol{\phi}_i\gamma_{ij}$, multiplying the above two equations by $\boldsymbol{\phi}_j^T$ and considering standard orthogonality conditions as well as the eigenvalue problem itself together with normalized modes $m_{jj} = \boldsymbol{\phi}_j^T\mathbf{M}\boldsymbol{\phi}_j = 1$, we are readily led to

$$\omega_j' = \frac{\kappa_{jj}'}{2\omega_j} = V_{gr} = \frac{d\omega_j}{dk}, \qquad \omega_j'' = \frac{1}{\omega_j}\left[\tfrac{1}{2}\kappa_{jj}'' - \omega_j'^2 - \sum_{n\neq j}\frac{\kappa_{jn}'\kappa_{nj}'}{\omega_n^2 - \omega_j^2}\right] \tag{B5a}$$

$$\gamma_{ij} = \frac{\kappa_{ij}'}{\omega_j^2 - \omega_i^2} = -\gamma_{ji}, \qquad \gamma_{jj} = 0 \tag{B5b}$$

$$\kappa_{ij}' = \boldsymbol{\phi}_i^T\mathbf{K}'\boldsymbol{\phi}_j = 2a_{ij}k + b_{ij} \qquad \kappa_{ij}'' = \boldsymbol{\phi}_i^T\mathbf{K}''\boldsymbol{\phi}_j = 2a_{ij} \tag{B5c}$$

$$a_{ij} = \boldsymbol{\phi}_i^T\mathbf{A}\boldsymbol{\phi}_j, \qquad b_{ij} = \boldsymbol{\phi}_i^T\mathbf{B}\boldsymbol{\phi}_j \tag{B5d}$$

Although the matrices in the eigenvalue problem are organized from top to bottom by interfaces, it is convenient for the purposes of our analysis –even if not for the solution of the eigenvalue problem itself– to organize these instead by degrees of freedom, separating the horizontal x from the vertical z degrees of freedom. After this is done, we are led to matrices and bilinear forms with the following structure:

$$\mathbf{A} = \begin{Bmatrix} \mathbf{A}_x & \mathbf{O} \\ \mathbf{O} & \mathbf{A}_z \end{Bmatrix}, \quad \mathbf{B} = \begin{Bmatrix} \mathbf{O} & \mathbf{B}_{xz} \\ \mathbf{B}_{zx} & \mathbf{O} \end{Bmatrix}, \quad \mathbf{G} = \begin{Bmatrix} \mathbf{G}_x & \mathbf{O} \\ \mathbf{O} & \mathbf{G}_z \end{Bmatrix}, \quad \mathbf{M} = \begin{Bmatrix} \mathbf{M}_x & \mathbf{O} \\ \mathbf{O} & \mathbf{M}_z \end{Bmatrix}, \quad \boldsymbol{\phi}_j = \begin{Bmatrix} \boldsymbol{\phi}_{xj} \\ \boldsymbol{\phi}_{zj} \end{Bmatrix} \tag{B6a}$$

$$a_{ij} = \boldsymbol{\phi}_{xi}^T\mathbf{A}_x\boldsymbol{\phi}_{xj} + \boldsymbol{\phi}_{zi}^T\mathbf{A}_z\boldsymbol{\phi}_{zj}, \qquad b_{ij} = \boldsymbol{\phi}_{xi}^T\mathbf{B}_{xz}\boldsymbol{\phi}_{zj} + \boldsymbol{\phi}_{zi}^T\mathbf{B}_{zx}\boldsymbol{\phi}_{xj} \tag{B6b}$$

It is further convenient to distinguish between longitudinal and transverse modes, which can be accomplished by means of Greek sub-indices α, β. Then, at the cutoff frequencies $k=0$, the modes uncouple into pure P and S modes for which $\boldsymbol{\phi}_{x\alpha} = \boldsymbol{\phi}_{z\beta} = \mathbf{0}$, in which case

$a_{\alpha\alpha} = \boldsymbol{\phi}_{z\alpha}^T \mathbf{A}_z \boldsymbol{\phi}_{z\alpha}$, $a_{\beta\beta} = \boldsymbol{\phi}_{x\beta}^T \mathbf{A}_x \boldsymbol{\phi}_{x\beta}$, $b_{\alpha\beta} = b_{\beta\alpha} = 2\boldsymbol{\phi}_{x\beta}^T \mathbf{B}_{xz} \boldsymbol{\phi}_{z\alpha}$, and $b_{\alpha\alpha} = b_{\beta\beta} = 0$. An exception to the latter identity is observed whenever two cutoff frequencies for P and S modes should coincide, a situation that can occur at isolated points when the ratio of wave velocities C_P / C_S is a rational number. In that case, the previous formula $b_{\alpha\beta} \neq 0$ would apply to that pair.

References

1) Mindlin, R.D. (1958a): "Waves and Vibrations in isotropic, elastic plates", *Structural Mechanics, Proceedings of the First Symposium on Naval Structural Mechanics*, held at Stanford University, California, August 11-14, 1958. Edited by J.N. Goodier and N.J. Hoff, Pergamon Press, New York, 1960.
2) Mindlin, R.D. (1958b): "Vibrations of an infinite, elastic plate at its cutoff frequencies", *Proceedings, Third U.S. National Congress of Applied Mechanics*, 225-226.
3) Prada, C. , Clorennec, D. and Royer, D. (2008a): "Local vibration of an elastic plate and zero-group velocity Lamb modes", *Journal of the Acoustical Society of America*, **124** (1), 203-212.
4) Prada, C., Clorennec, D., and Royer, D. (2008b) : "Power law decay of zero group velocity Lamb modes", *Wave Motion*, **45**, 723-738.
5) Prada, C. , Clorennec, D. and Royer, D. (2009): "Influence of Anisotropy on zero-group velocity Lamb modes", *Journal of the Acoustical Society of America*, **126** (2), 620-625.
6) Cès, M. , Clorennec, D., Royer, D. and Prada, C. (2011): "Edge resonance and zero group velocity Lamb modes in a free elastic plate", *Journal of the Acoustical Society of America*, **130** (2), 620-625.
7) Tassoulas, J.L., and Akylas, T.R. (1984): "On wave modes with zero group velocity in an elastic layer", *Journal of Applied Mechanics*, ASME, **51** (September), 652-656.
8) Kausel, E. (2006): *Fundamental Solutions in Elastodynamics: A Compendium*, Cambridge University Press.
9) Waas, G. (1972): "Linear two-dimensional analysis of soil dynamic problems in semi-infinite layer media", *PhD Thesis*, University of California, Berkeley.
10) Kausel, E. and Peek, R. (1982): "Dynamic loads in the interior of a layered stratum: An explicit solution", *Bull. Seism. Soc. Am.*, **72** (5), 1459-1481 (see also the Errata in *BSSA*, **74**, Aug. 1984. p. 1508).
11) Kausel, E. (1986): "Wave Propagation in Anisotropic Layered Media", *International Journal for Numerical Methods in Engineering*, **23**:1567 1578.
12) Kausel, E. (1994): "Thin-layer Method: Formulation in the time domain", *Int. J. Num. Meth. Eng.*, 37, 927-941.